

# JOURNAL OF THE AMERICAN CHEMICAL SOCIETY

© Copyright 1988 by the American Chemical Society

VOLUME 110, NUMBER 23

NOVEMBER 9, 1988

## The Interaction of Formamide with Hydrogen-Presaturated Ru(001): Conversion of $\eta^1(\text{O})\text{-NH}_2\text{CHO}$ to $\eta^2(\text{C,O})\text{-Bonded}$ Species

J. E. Parmeter<sup>†</sup> and W. H. Weinberg\*

*Contribution from the Division of Chemistry and Chemical Engineering, California Institute of Technology, Pasadena, California 91125. Received January 11, 1988*

**Abstract:** Both the adsorption and the decomposition of formamide ( $\text{NH}_2\text{CHO}$ ) have been studied on a hydrogen-presaturated ( $\theta_{\text{H}} \sim 0.85$ ) Ru(001) surface using high-resolution electron energy loss spectroscopy and thermal desorption mass spectrometry. At a surface temperature of 80 K, the formamide chemisorbs molecularly via an electron lone pair on the oxygen atom in an  $\eta^1(\text{O})\text{-NH}_2\text{CHO}$  configuration. The  $\eta^1(\text{O})\text{-NH}_2\text{CHO}$  undergoes competing desorption and conversion to  $\eta^2(\text{C,O})\text{-NH}_2\text{CHO}$  [and possibly some  $\eta^2(\text{C,O})\text{-NH}_2\text{CO}$  also] below 225 K, with only conversion to  $\eta^2(\text{C,O})\text{-NH}_2\text{CHO}$  occurring for sufficiently low formamide coverages. Further annealing of the surface to 250 K causes the  $\eta^2(\text{C,O})\text{-NH}_2\text{CHO}$  to undergo carbon-hydrogen bond cleavage to produce  $\eta^2(\text{C,O})\text{-NH}_2\text{CO}$ , and this species decomposes below 300 K to produce CO, additional hydrogen adatoms, and NH. The NH decomposes near 400 K to nitrogen and hydrogen adatoms, and the desorption of the following reaction products (approximate peak desorption temperatures) is observed: CO (450 K),  $\text{H}_2$  (305, 360, and 405 K), and  $\text{N}_2$  (770 K). Following a saturation formamide exposure, approximately 0.05 monolayer of formamide decomposes on the hydrogen-presaturated surface.

### I. Introduction

The interactions of organic molecules containing more than one double bond and/or a heteroatom with well-defined transition metal surfaces under ultrahigh vacuum (UHV) conditions has been the subject of much study recently.<sup>1</sup> These molecules are of particular interest because several bonding configurations are possible for the adsorbed molecule, such as  $\pi$ - or di- $\sigma$ -bonding via the molecular double bond or  $\sigma$ -donor bonding via a heteroatom electron lone pair. The electronic structure of the substrate (i.e., the metal surface) is manifest in the nature of (molecular) ligand bonding and in the reactions that the ligand undergoes, just as the electronic properties of a catalyst surface are manifest in the rates and mechanisms of its catalytic reactions. Studies of the adsorption of such molecules can possibly identify surface intermediates which may be involved in high-pressure heterogeneously catalyzed surface reactions, but which cannot be identified directly under reaction conditions due to their low steady-state concentrations. In addition, the intermediates identified on transition metal surfaces and their stability can be compared with those in organometallic compounds, thus rendering more systematic the connection between surface chemistry and organometallic chemistry. We have reported recently the results of studies of formamide adsorption and decomposition both on the clean Ru(001) surface<sup>2</sup> and on the Ru(001) surface that is modified chemically by an ordered  $p(1 \times 2)$  overlayer of oxygen adatoms ( $\theta_0 = 0.5$ , where  $\theta = 1$  corresponds to a surface concentration of  $1.58 \times 10^{15} \text{ cm}^{-2}$ ).<sup>3,4</sup> We report here the results of a study of the adsorption and decomposition of formamide on

a Ru(001) surface with a saturation precoverage of hydrogen adatoms. Hydrogen adatoms are a product of the decomposition of formamide on clean Ru(001), and could alter both the products of formamide decomposition and their stability.

Our previous studies of formamide on the Ru(001) and Ru(001)- $p(1 \times 2)\text{-O}$  surfaces showed that the presence of the  $p(1 \times 2)$  oxygen adatom overlayer alters profoundly the chemistry of this molecule on this hexagonally close-packed ruthenium surface. The principal decomposition mechanisms of formamide on the clean and oxygen-precovered surfaces are shown in Figure 1. On clean Ru(001), the principal bonding configuration of formamide at 80 K involves CH bond cleavage and rehybridization of the CO double bond to produce an  $\eta^2(\text{C,O})\text{-NH}_2\text{CO}$  species;<sup>5</sup> this species decomposes at higher temperatures to give a mixture of coadsorbed CO, NH,  $\text{NH}_3$ , and hydrogen adatoms. On the Ru(001)- $p(1 \times 2)\text{-O}$  surface at 80 K, formamide adsorbs molecularly in an  $\eta^1(\text{O})\text{-bonded}$  configuration, via an electron lone pair on the oxygen atom of the formamide. The subsequent decomposition is via a formate-like  $\eta^2(\text{N,O})\text{-NHCHO}$  intermediate, and only 0.05 monolayer of formamide decomposes [as opposed to 0.15 mono-

(1) See, for example, ref 36 and 37 below, and references therein, as well as a number of additional references in ref 4.

(2) Parmeter, J. E.; Schwalke, U.; Weinberg, W. H. *J. Am. Chem. Soc.* **1988**, *110*, 53.

(3) Parmeter, J. E.; Schwalke, U.; Weinberg, W. H. *J. Am. Chem. Soc.* **1987**, *109*, 1876.

(4) Parmeter, J. E.; Schwalke, U.; Weinberg, W. H. *J. Am. Chem. Soc.* **1987**, *109*, 5083.

(5) There is a second, minor decomposition mechanism for formamide on clean Ru(001) at high coverage. See ref 2 for details.

<sup>†</sup> AT&T Bell Laboratories Predoctoral Fellow.

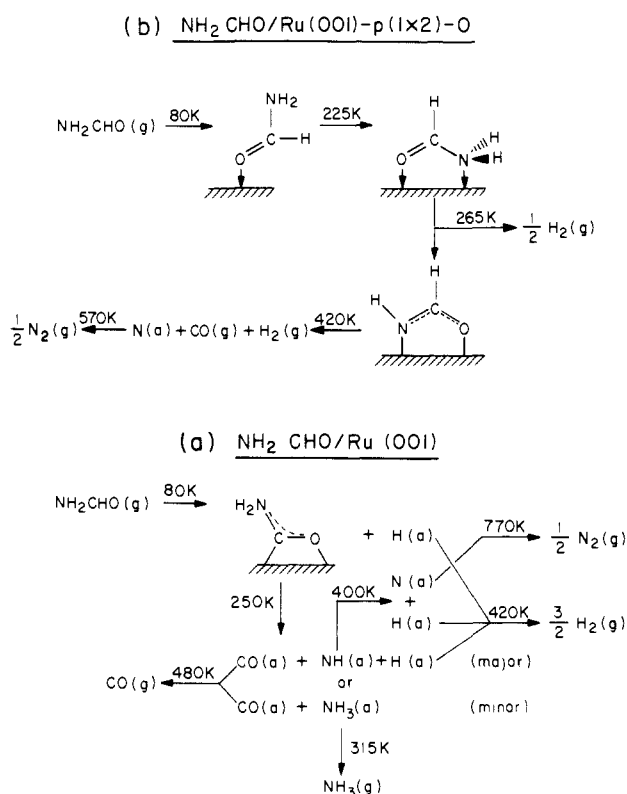


**Figure 1.** The principal decomposition mechanisms of formamide (a) on the Ru(001) surface with an ordered  $p(1\times 2)$  overlayer of oxygen adatoms ( $\theta_0 = 0.5$ ) and (b) on clean Ru(001). The NH and  $\text{NH}_3$  that are formed from  $\eta^2(\text{C},\text{O})\text{-NH}_2\text{CHO}$  decomposition on clean Ru(001) are probably formed via the dehydrogenation and hydrogenation of a short-lived  $\text{NH}_2$  species which results upon carbon–nitrogen bond cleavage of  $\eta^2(\text{C},\text{O})\text{-NH}_2\text{CHO}$ , but the  $\text{NH}_2$  is not spectroscopically identified.

layer on clean Ru(001)]. The effects of preadsorbed hydrogen on the surface chemistry of formamide are of interest, for example, because a large precoverage of hydrogen adatoms may present the same steric barriers to the reaction of formamide that oxygen adatoms do, but without producing the same clear-cut electronic (i.e., electron-withdrawing) effects.

In order to understand the reactions of formamide on a hydrogen-presaturated Ru(001) surface, it is necessary to study first the properties of hydrogen alone on Ru(001). A number of studies have dealt with this subject.<sup>6–12</sup> At all temperatures investigated to date ( $T \geq 80$  K), hydrogen adsorbs dissociatively on Ru(001). The hydrogen adatoms occupy threefold hollow sites exclusively, and no ordered overlayers are known to form at any coverage. The saturation coverage of hydrogen adatoms has been estimated to be  $0.85 \pm 0.15$  monolayer.<sup>6</sup> When the hydrogen-saturated Ru(001) surface is annealed, recombinative desorption of  $\text{H}_2$  occurs between approximately 275 and 425 K, with a maximum desorption rate near 320 K and a shoulder near 380 K.<sup>6,9</sup> At saturation coverage, hydrogen adatoms give rise to two very weak EELS features near 840 and 1135  $\text{cm}^{-1}$ , which are due respectively to the asymmetric and symmetric ruthenium–hydrogen stretching modes.<sup>8,10</sup> Both of these loss features are sufficiently weak that they often cannot be observed when other surface species are present that give rise to loss features in the same frequency range.

The organometallic chemistry of formamide and related ligands containing an NCO group has received considerable attention recently.<sup>13–33</sup> The ligands  $\eta^1(\text{O})\text{-NH}_2\text{CHO}$ ,  $\eta^2(\text{C},\text{O})\text{-NH}_2\text{CHO}$ ,

and  $\eta^2(\text{C},\text{O})\text{-NH}_2\text{CO}$  are of particular relevance to the present study. Compounds containing  $\eta^1(\text{O})$ -bonded amide ligands have been synthesized and characterized in which the metal atom is Pt(II)<sup>13</sup> and Co(III).<sup>14</sup> The latter complex,  $(\text{NH}_3)_5\text{Co}(\text{NH}_2\text{CHO})^{3+}$ , has a carbon–oxygen stretching frequency of 1675  $\text{cm}^{-1}$ , in good agreement with that of 1660  $\text{cm}^{-1}$  of  $\eta^1(\text{O})\text{-NH}_2\text{CHO}$  on Ru(001)– $p(1\times 2)\text{-O}$ .<sup>3,4</sup> A number of compounds of ruthenium- and osmium-containing  $\eta^2(\text{C},\text{O})\text{-NR}_2\text{CO}$  ( $\text{R} = \text{H}$  or alkyl) ligands have been synthesized,<sup>19–24</sup> and while some infrared data are available, mode assignments have not, to our knowledge, been given. We know of no organometallic analogues of  $\eta^2(\text{C},\text{O})\text{-NH}_2\text{CHO}$ , although analogous  $\eta^2(\text{C},\text{O})$ -bonded formaldehyde<sup>34</sup> and acetone<sup>35</sup> ligands have been identified in organometallic compounds, and  $\eta^2(\text{C},\text{O})\text{-H}_2\text{CO}$ <sup>36</sup> and  $\eta^2(\text{C},\text{O})\text{-(CH}_3)_2\text{CO}$ <sup>37</sup> have been identified previously on Ru(001). Both on the Ru(001) surface and in the organometallic compounds, these ligands have carbon–oxygen stretching frequencies between 1000 and 1300  $\text{cm}^{-1}$ .

## II. Experimental Details

The experimental techniques employed in this study were high-resolution electron energy loss spectroscopy (EELS) and thermal desorption mass spectrometry (TDMS). The EELS and TDMS experiments were performed in an UHV chamber that has been described in detail elsewhere.<sup>38</sup> The home-built EEL spectrometer is of the Kuyatt–Simpson

- (13) Meester, M. A. M.; Stufkens, D. J.; Vrieze, K. *Inorg. Chim. Acta* **1976**, *16*, 191.
- (14) Balahura, R. J.; Jordan, R. B. *J. Am. Chem. Soc.* **1970**, *92*, 1533.
- (15) Sacco, A.; Giannoccaro, P.; Vasapoloo, G. *Inorg. Chim. Acta* **1984**, *83*, 125.
- (16) Kruse, A. E.; Angelici, R. J. *J. Organomet. Chem.* **1970**, *24*, 231.
- (17) Behrens, H.; Jungbauer, A. *Z. Naturforsch. B* **1979**, *34*, 1477.
- (18) Lindsay, A. J.; Kim, S.; Jacobson, R. A.; Angelici, R. J. *Organometallics* **1984**, *3*, 1523.
- (19) Szostak, R.; Strouse, C. E.; Kaesz, H. D. *J. Organomet. Chem.* **1980**, *191*, 243.
- (20) Mayr, A.; Lin, Y.-C.; Boag, N. M.; Kaesz, H. D. *Inorg. Chem.* **1982**, *21*, 1704.
- (21) Kampe, C. E.; Boag, N. M.; Kaesz, H. D. *J. Mol. Catal.* **1983**, *21*, 297.
- (22) Fagan, P. J.; Manriquez, J. M.; Vollmer, S. H.; Day, C. S.; Day, V. W.; Marks, T. J. *J. Am. Chem. Soc.* **1981**, *103*, 2206.
- (23) Yasuda, H.; Araki, T.; Tani, H. *J. Organomet. Chem.* **1973**, *49*, 103.
- (24) Azam, K. A.; Yin, C. C.; Deeming, A. J. *J. Chem. Soc., Dalton Trans.* **1978**, 1201.
- (25) Rossi, R.; Duatti, A.; Magon, L.; Casellato, U.; Graziani, R.; Toniolo, L. *Inorg. Chim. Acta* **1983**, *74*, 77.
- (26) Sahajpal, A.; Robinson, R. D. *Inorg. Chem.* **1979**, *18*, 3572.
- (27) Schwering, H.-U.; Weidlein, J. *Chimia* **1973**, *27*, 535.
- (28) Jennings, J. R.; Wade, K.; Wyatt, B. K. *J. Chem. Soc. A* **1968**, 2535.
- (29) Adams, R. D.; Golembeski, N. M. *J. Organomet. Chem.* **1979**, *171*, C21.
- (30) Adams, R. D.; Golembeski, N. M.; Selegue, J. P. *Inorg. Chem.* **1981**, *20*, 1242.
- (31) Lin, Y. C.; Knobler, C. B.; Kaesz, H. D. *J. Am. Chem. Soc.* **1981**, *103*, 1216.
- (32) Kaesz, H. D.; Knobler, C. B.; Andrews, M. A.; van Buskirk, G.; Szostak, R.; Strouse, C. E.; Lin, Y. C.; Mayr, A. *Pure Appl. Chem.* **1982**, *54*, 131.
- (33) Burgess, K.; Johnson, B. F. G.; Lewis, J. J. *J. Chem. Soc., Dalton Trans.* **1983**, 1179.
- (34) (a) Brown, K. L.; Clark, G. R.; Headford, C. E. L.; Marsden, K.; Roper, W. R. *J. Am. Chem. Soc.* **1979**, *101*, 503. (b) Gambarotta, S.; Floriani, C.; Chiesi-Villa, A.; Gaustini, C. *J. Am. Chem. Soc.* **1982**, *104*, 2019.
- (c) Buhro, W. E.; Patton, A. T.; Strouse, C. E.; Gladysz, J. A.; McCormick, F. B.; Etter, M. C. *J. Am. Chem. Soc.* **1983**, *105*, 1056.
- (35) (a) Countryman, R.; Penfold, B. R. *J. Cryst. Mol. Struct.* **1972**, *2*, 281. (b) Tsou, T. T.; Huffman, J. C.; Kochi, J. K. *Inorg. Chem.* **1979**, *18*, 2311. (c) Additional references in ref 37a.
- (36) Anton, A. B.; Parmeter, J. E.; Weinberg, W. H. *J. Am. Chem. Soc.* **1985**, *107*, 5558; **1986**, *108*, 1823.
- (37) (a) Avery, N. R.; Anton, A. B.; Toby, B. H.; Weinberg, W. H. *J. Electron Spectrosc. Relat. Phenom.* **1983**, *29*, 233. (b) Avery, N. R.; Weinberg, W. H.; Anton, A. B.; Toby, B. H. *Phys. Rev. Lett.* **1983**, *51*, 682. (c) Anton, A. B.; Avery, N. R.; Toby, B. H.; Weinberg, W. H. *J. Am. Chem. Soc.* **1986**, *108*, 684.
- (38) Thomas, G. E.; Weinberg, W. H. *Rev. Sci. Instrum.* **1979**, *50*, 497.

(6) Shimizu, H.; Christmann, K.; Ertl, G. *J. Catal.* **1980**, *61*, 412.

(7) Barteau, M. A.; Broughton, J. Q.; Menzel, D. *Surf. Sci.* **1983**, *133*, 443.

(8) Conrad, H.; Scala, R.; Stenzel, W.; Unwin, R. *J. Chem. Phys.* **1984**, *81*, 6371.

(9) Feulner, P.; Menzel, D. *Surf. Sci.* **1985**, *154*, 465.

(10) Feibelman, P. J.; Hamann, D. R. *Surf. Sci.* **1985**, *149*, 48.

(11) Hrbek, J. *J. Catal.* **1986**, *100*, 523.

(12) Hrbek, J. *J. Phys. Chem.* **1986**, *90*, 6217.

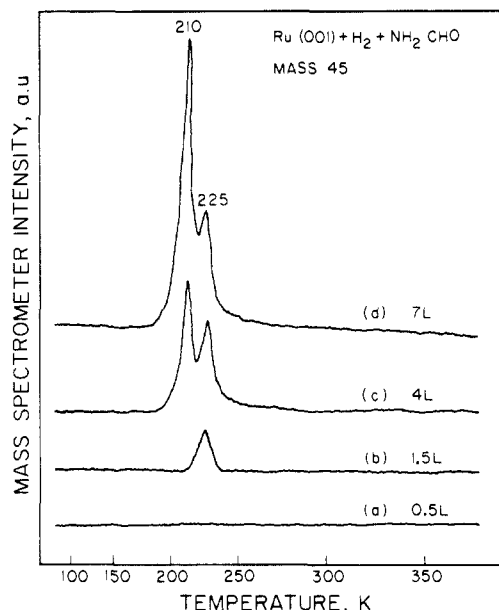


Figure 2. Thermal desorption spectra of molecular formamide ( $m/e = 45$  amu) following various exposures of formamide to a hydrogen-presaturated Ru(001) surface at 80 K.

type, with electrostatic hemispheres serving as the energy dispersing elements in both the monochromator and analyzer. Typical experimental parameters for the EELS measurements were the following: impact energy, approximately 4 eV; resolution (full-width at half-maximum of the elastically scattered beam),  $75 \text{ cm}^{-1}$ ; count rate,  $2 \times 10^5$  cps in the elastically scattered beam; and (fixed) angle of incidence of the incident electron beam,  $60^\circ$  with respect to the surface normal. All EEL spectra were measured with electron collection in the specular direction, except as noted. The EEL spectra were measured after annealing the crystal at a rate of approximately  $10 \text{ K-s}^{-1}$  to an indicated temperature with immediate recoiling of the surface to 80 K.

The UHV chamber was pumped by a  $220 \text{ L-s}^{-1}$  Varian noble vacuum pump and a titanium sublimation pump. The background pressure was below  $2 \times 10^{-10}$  torr during all EELS measurements, and the base pressure was below  $5 \times 10^{-11}$  torr. Liquid nitrogen cooling allowed crystal temperatures as low as 80 K to be obtained routinely. The Ru(001) crystal was cleaned by annealing cycles between 1100 and 1500 K in a background of  $5 \times 10^{-8}$  torr of  $\text{O}_2$ , followed by annealing to 1650 K in vacuo. Occasionally, argon ion sputtering was also employed (1 keV, 1–2  $\mu\text{A}$  current at the crystal for 2–3 h). The Ru(001) surface was judged to be clean when it exhibited both a featureless EEL spectrum and  $\text{H}_2$  thermal desorption spectra that are characteristic of the clean surface.<sup>6,9</sup>

The UHV chamber also contained a quadrupole mass spectrometer for performing thermal desorption measurements and for monitoring the purity of the gases introduced into the UHV chamber. All thermal desorption spectra were obtained with a heating rate of 6–10  $\text{K-s}^{-1}$ . Exposures were effected by backfilling the UHV chamber through leak valves. The formamide used in this study was obtained from Aldrich (reported minimum purity of 99%), and the hydrogen was obtained from Matheson (reported minimum purity of 99.9995%). The detailed procedure of admitting formamide into the UHV chamber has been discussed elsewhere.<sup>4</sup>

### III. Results

**A. Thermal Desorption Mass Spectrometry.** The clean Ru(001) surface at 80 K can be nearly saturated with hydrogen adatoms [ $\theta_{\text{H}} \approx 0.85^6$ ] by exposure to 5 L (1 L  $\equiv$  1 Langmuir  $\equiv 10^{-6}$  torr-s) or more of  $\text{H}_2$ . When the hydrogen-presaturated surface is exposed to various fluxes of  $\text{NH}_2\text{CHO}$  at 80 K, the following species are detected in subsequent TDM spectra:  $\text{NH}_2\text{CHO}$ , CO,  $\text{H}_2$ , and  $\text{N}_2$ . The exposures quoted below were measured with an ionization gauge, and are uncorrected for the relative ionization probabilities of the various gases.

Figure 2 shows molecular  $\text{NH}_2\text{CHO}$  thermal desorption spectra ( $m/e = 45$  amu) following various exposures of  $\text{NH}_2\text{CHO}$  to the hydrogen-presaturated Ru(001) surface at 80 K. For a 0.5-L exposure, no molecular desorption occurs, indicating that all of the adsorbed formamide decomposes upon heating. For exposures

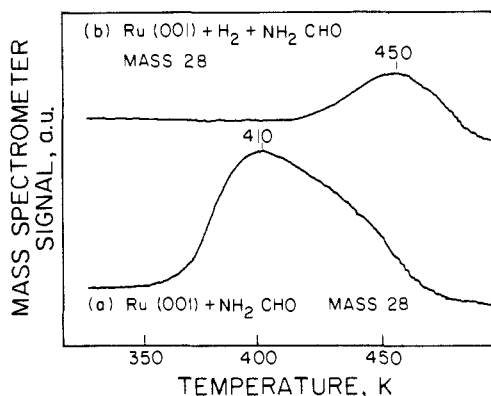


Figure 3. Thermal desorption spectra of CO ( $m/e = 28$  amu) following saturation (8 L) formamide exposures on (a) clean Ru(001) at 80 K, and (b) a hydrogen-presaturated [10 L of  $\text{H}_2$  exposure] Ru(001) surface at 80 K.

greater than 1 L, a desorption peak appears at 225 K; for exposures greater than approximately 2.5 L, a second desorption peak appears at 210 K, the latter of which does not saturate with increasing exposures. In agreement with the results of our previous studies of formamide adsorption on clean Ru(001) and Ru(001)- $p(1 \times 2)$ -O,<sup>2,4</sup> the 210-K peak is attributed to the desorption of condensed formamide multilayers, while the 225-K peak is due to the desorption of monolayer formamide. The temperatures of these two desorption peaks and the amount of formamide that desorbs in the 225-K peak are nearly identical within experimental error for both the clean and the hydrogen-presaturated surface. Both peaks appear at a lower exposure, however, on the hydrogen-presaturated surface.

Thermal desorption spectra of CO ( $m/e = 28$  amu) are shown in Figure 3 for saturation  $\text{NH}_2\text{CHO}$  exposures on both clean and hydrogen-presaturated Ru(001). A single CO thermal desorption peak is observed in each case, at 410 K on the clean surface (a), and at 450 K on the hydrogen-covered surface (b). On the clean surface, the CO thermal desorption peak occurs at 480 K following a 0.5-L  $\text{NH}_2\text{CHO}$  exposure and shifts downward continuously to 410 K at saturation.<sup>2</sup> The downshift is much less pronounced on the hydrogen-precovered surface (from 470 to 450 K) consistent with the lower formamide coverages that are involved. Both EEL spectra [cf. section III.B] and previous thermal desorption measurements following CO adsorption on Ru(001)<sup>39</sup> show clearly that the thermal desorption spectra of Figure 3 result from molecularly adsorbed CO, rather than from the recombination and desorption of carbon and oxygen adatoms.<sup>40</sup> The amount of CO that is desorbed following a saturation  $\text{NH}_2\text{CHO}$  exposure on hydrogen-presaturated Ru(001) allows the fractional surface coverage of formamide that decomposes to be estimated as approximately 0.05 monolayer, compared with 0.15 monolayer on the initially clean surface and 0.05 monolayer on Ru(001)- $p(1 \times 2)$ -O. The coverage of 0.05 monolayer corresponds to approximately  $8 \times 10^{13}$  formamide molecules- $\text{cm}^{-2}$ .<sup>41</sup>

Figure 4 shows hydrogen thermal desorption spectra ( $m/e = 2$  amu) for a hydrogen-saturated Ru(001) surface (a), and for a hydrogen-saturated Ru(001) surface that has been exposed to 6 L of  $\text{NH}_2\text{CHO}$  (b). As noted previously, thermal desorption spectra of  $\text{H}_2$  from hydrogen-saturated Ru(001) show a peak at 320 K with a shoulder near 380 K. Thermal desorption spectra of  $\text{H}_2$  from the hydrogen-presaturated surface with coadsorbed  $\text{NH}_2\text{CHO}$  show a desorption maximum at 305 K, a pronounced shoulder at 360 K, and a weak shoulder at 405 K. As in the case of the decomposition of formamide on clean Ru(001),<sup>2</sup> the re-

(39) (a) Madey, T. E.; Menzel, D. *J. Appl. Phys., Suppl. 2 Pt.* **1974**, *2*, 229. (b) Pfnür, H.; Feulner, P.; Engelhardt, H. A.; Menzel, D. *Chem. Phys. Lett.* **1978**, *59*, 481. (c) Pfnür, H.; Feulner, P.; Menzel, D. *J. Chem. Phys.* **1983**, *79*, 4613.

(40) The recombinative desorption of carbon and oxygen adatoms, evolving CO, occurs with a maximum rate near 650 K on this surface: Hills, M. M.; Parmeter, J. E.; Weinberg, W. H. *J. Am. Chem. Soc.* **1987**, *109*, 4224.

(41) The density of surface ruthenium atoms is  $1.58 \times 10^{15} \text{ cm}^{-2}$ .

**Table I.** Vibrational Frequencies (in  $\text{cm}^{-1}$ ) and Mode Assignments for Various Formamide-Derived Species on Ru(001)-p(1 $\times$ 2)-O, Hydrogen-Presaturated Ru(001) ( $\theta_{\text{H}} \approx 0.85$ ), and Clean Ru(001)<sup>a</sup>

mode	NH <sub>2</sub> CHO		$\eta^1(\text{O})\text{-NH}_2\text{CHO}$		$\eta^2(\text{C,O})\text{-NH}_2\text{CHO}$	$\eta^2(\text{C,O})\text{-NH}_2\text{CO}$
	gas (44)	liquid (43)	Ru(001)-p(1 $\times$ 2)-O $\theta_0 = 0.5$ (4) <sup>b</sup>	Ru(001) + H (this work) <sup>b</sup>	Ru(001) + H (this work) <sup>c</sup>	Ru(001) (2)
$\nu_s(\text{NH}_2)$	3545	3330	3490	3500	3335	3510 <sup>d</sup>
$\nu_s(\text{NH}_2)$	3451	3190	3230	3220		3380 <sup>d</sup>
$\nu(\text{CH})$	2852	2882	2940	2945	2890	
$\nu(\text{CO})$	1734	1690	1660	1670	<i>e</i>	<i>d</i>
$\delta(\text{NH}_2)$	1572	1608	1585	1585	<i>e</i>	<i>e</i>
$\nu(\text{CN})$	1255	1309			<i>e</i>	<i>e</i>
			1360	1355		
$\delta(\text{CH})$	1378	1391			n.o.	
$\pi(\text{CH})$	1030	1056	n.o.	n.o.	1135	
$\rho(\text{NH}_2)$	1059	1090	1110	1115	<i>e</i>	<i>e</i>
$\omega(\text{NH}_2)$	289(?)	750	790	795	825	820
$\tau(\text{NH}_2)$	602	200	n.o.	670(?)	n.o.	n.o.
$\delta(\text{NCO})$	565	608	525	525	655	655
$\nu(\text{Ru-ligand})$			300	n.o.	300, 445	270, 360

<sup>a</sup>Data for gas-phase and liquid formamide are given for comparison. *a* = asymmetric, *s* = symmetric, n.o. = not observed. References are given in parentheses. <sup>b</sup>These frequencies are based on 0.5-L formamide exposures. At higher coverages, some frequency shifts are observed due to hydrogen-bonding among the adsorbed molecules. <sup>c</sup>These vibrational frequencies are based on the EEL spectrum of Figure 6a, in which some  $\eta^2(\text{C,O})\text{-NH}_2\text{CO}$  may also be present. <sup>d</sup>These modes are well-resolved only in off-specular spectra. <sup>e</sup>In the case of  $\eta^2(\text{C,O})\text{-NH}_2\text{CHO}$ , modes occur with frequencies of 1585, 1395, 1300, and 1015  $\text{cm}^{-1}$ , which are due to  $\delta(\text{NH}_2)$ ,  $\rho(\text{NH}_2)$ ,  $\nu_s(\text{NCO})$ , and  $\nu_s(\text{NCO})$ . Since coupling among these modes is significant, specific assignments cannot be given. The situation is similar for  $\eta^2(\text{C,O})\text{-NH}_2\text{CO}$ , which on clean Ru(001) exhibits loss features at 1580, 1370, 1300, and 1015  $\text{cm}^{-1}$ .

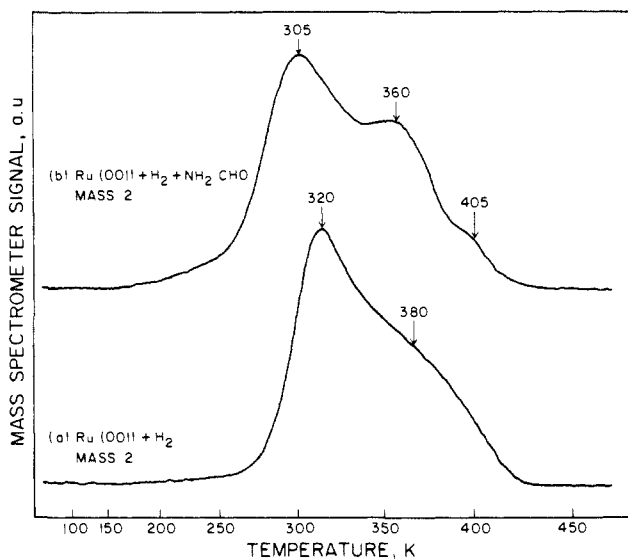


**Figure 4.** Thermal desorption spectra of H<sub>2</sub> ( $m/e = 2$  amu) from a Ru(001) surface that has been exposed to (a) 10 L of H<sub>2</sub> (saturation) at 80 K, and (b) 10 L of H<sub>2</sub> followed by 8 L of NH<sub>2</sub>CHO at 80 K.

combinative desorption of molecular nitrogen ( $m/e = 28$  amu, with a cracking fragment at  $m/e = 14$  amu) is observed. The range of desorption temperatures (approximately 740–810 K) and the peak temperature (approximately 770–790 K) are similar for similar coverages of irreversibly adsorbed formamide in the two cases.

**B. Electron Energy Loss Spectroscopy.** As noted previously, the adsorption of hydrogen on Ru(001) leads to the appearance of two very weak loss features near 840 and 1125  $\text{cm}^{-1}$ . These are due to the asymmetric and symmetric ruthenium–hydrogen stretching modes, respectively, of hydrogen adatoms adsorbed in threefold hollow sites. The EEL spectrum of Figure 5a is observed when the hydrogen-presaturated surface is exposed to 0.5 L of NH<sub>2</sub>CHO at 80 K. For comparison, Figure 5b shows the EEL spectrum that results when the Ru(001) surface with an ordered p(1 $\times$ 2) overlayer of oxygen adatoms ( $\theta_0 = 0.5$ ) is exposed to 0.5 L of NH<sub>2</sub>CHO at 80 K.<sup>3,4</sup> Although there are slight differences in the frequencies and relative intensities of some loss features, it is clear that the same surface species is formed in both cases. This species has been identified previously as  $\eta^1(\text{O})\text{-NH}_2\text{CHO}$ , molecularly chemisorbed formamide that is bonded to the surface

via a lone pair of electrons on the oxygen atom of the formamide.<sup>3,4</sup> The mode assignments for this species are given in Table I, and the frequencies compare well to those of liquid<sup>43</sup> gas-phase<sup>44</sup> formamide. The carbonyl stretching frequency of 1670  $\text{cm}^{-1}$  is characteristic of a carbon–oxygen double bond and indicates that no significant rehybridization of this bond has occurred. The assignment of the various NH<sub>2</sub> modes has been confirmed for  $\eta^1(\text{O})\text{-NH}_2\text{CHO}$  on the Ru(001)-p(1 $\times$ 2)-O surface by measuring EEL spectra of adsorbed ND<sub>2</sub>CHO.<sup>4</sup> The identity of the weak loss feature at 670  $\text{cm}^{-1}$  in Figure 5a is uncertain, but it is possibly due to  $\tau(\text{NH}_2)$ . The loss features at 795 and 1115  $\text{cm}^{-1}$  are too intense to be attributed solely to the ruthenium–hydrogen stretching modes of the coadsorbed hydrogen adatoms. The broad feature at 570  $\text{cm}^{-1}$  in Figure 5b is due to two overlapping loss features:  $\delta(\text{NCO})$  of  $\eta^1(\text{O})\text{-NH}_2\text{CHO}$  at 525  $\text{cm}^{-1}$ , and  $\nu_s(\text{RuO})$  of the coadsorbed oxygen adatoms at 585  $\text{cm}^{-1}$ . Neither spectrum in Figure 5 shows evidence for any formamide decomposition after adsorption at 80 K. The very weak loss feature near 2000  $\text{cm}^{-1}$  in both spectra is due to less than 0.005 monolayer of carbon monoxide adsorbed from the chamber background.<sup>42</sup>

The EEL spectra of Figure 5, c and d, result when the hydrogen-presaturated Ru(001) surface at 80 K is exposed to 2 and 4 L of formamide, respectively. Note by comparison to Figure 2 that while Figure 5a corresponds to a coverage where no formamide desorbs molecularly, Figure 5c corresponds to a coverage where some formamide desorbs molecularly in the 225-K desorption peak, and Figure 5d corresponds to a coverage where multilayer formamide is present. The EEL spectrum of Figure 5c is also characteristic of  $\eta^1(\text{O})$ -bonded formamide, but due to the increased coverage it shows some pronounced differences compared with Figure 5a. The most noticeable difference is the very intense, broadened and downshifted  $\omega(\text{NH}_2)$  loss feature at 710  $\text{cm}^{-1}$ , and the NH<sub>2</sub> stretching region shows a broad, multi-peaked structure. These changes are attributable to hydrogen-bonding among the adsorbed formamide molecules.<sup>43</sup> The EEL spectrum of Figure 5d shows similar changes, as well as an intense loss at 215  $\text{cm}^{-1}$  due to a lattice mode of the formamide multilayers. A loss feature at 2400  $\text{cm}^{-1}$  is also observed, which is due to a combination band of the loss features at 710 and 1695  $\text{cm}^{-1}$ . Similar changes in the EEL spectra of formamide on Ru-

(42) (a) Thomas, G. E.; Weinberg, W. H. *J. Chem. Phys.* **1978**, *69*, 3611. (b) Pfnür, H.; Menzel, D.; Hoffmann, F. M.; Ortega, A.; Bradshaw, A. M. *Surf. Sci.* **1980**, *93*, 431.

(43) Suzuki, I. *Bull. Chem. Soc. Jpn.* **1960**, *33*, 1359.

(44) (a) Evans, J. C. *J. Chem. Phys.* **1954**, *22*, 1228. (b) King, S. T. *J. Phys. Chem.* **1971**, *75*, 405.

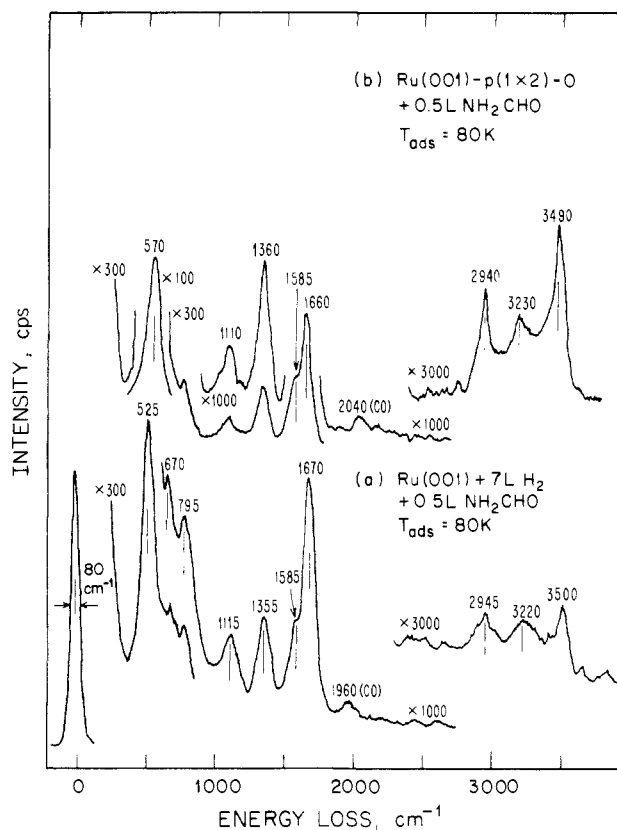
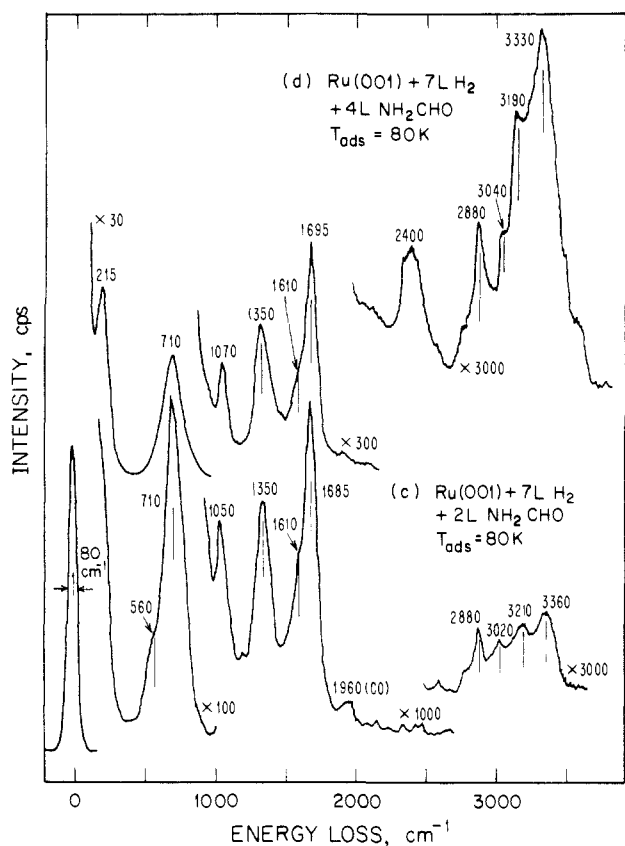


**Figure 5.** The EEL spectra that result following (a) a 0.5-L NH<sub>2</sub>CHO exposure to hydrogen-saturated Ru(001), (b) a 0.5-L NH<sub>2</sub>CHO exposure to Ru(001)-p(1×2)-O, (c) 2-L NH<sub>2</sub>CHO exposure to hydrogen-saturated Ru(001), and (d) a 4-L NH<sub>2</sub>CHO exposure to hydrogen-saturated Ru(001). All exposures were made, and all EEL spectra measured, with the surface held at a temperature of 80 K.

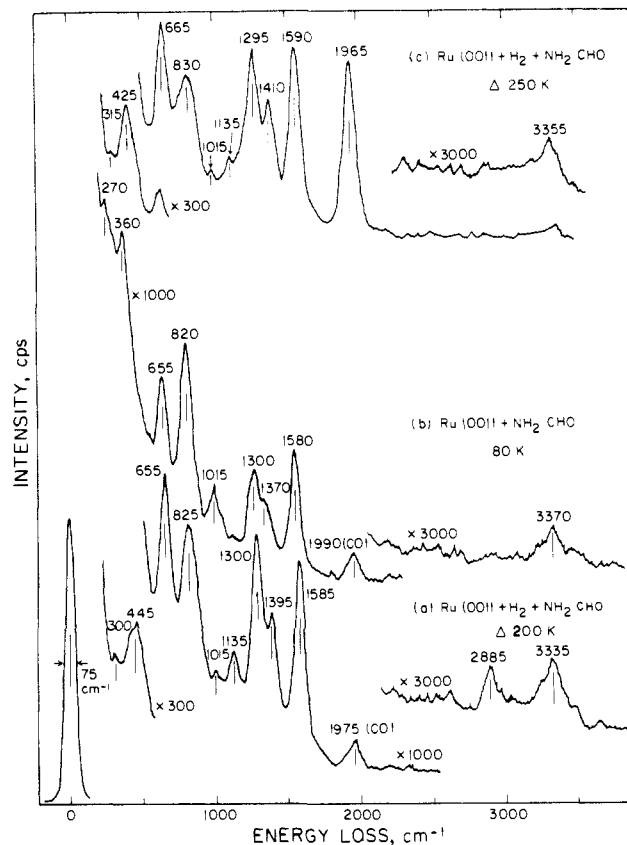


**Figure 6.** The EEL spectra that result from the following treatments of a Ru(001) surface: (a) 10 L of H<sub>2</sub> followed by 0.5 L of NH<sub>2</sub>CHO and annealed to 200 K; (b) 0.5 L of NH<sub>2</sub>CHO; and (c) 10 L of H<sub>2</sub> followed by 0.5 L of NH<sub>2</sub>CHO and annealed to 250 K. All exposures were made, and all EEL spectra measured, with the surface held at a temperature of 80 K.

(001)-p(1×2)-O at 80 K were also observed as the exposure was increased.<sup>4</sup>

Annealing the Ru(001) surface represented by Figure 5a briefly to 150 K<sup>45</sup> causes the partial conversion of  $\eta^1(\text{O})\text{-NH}_2\text{CHO}$  to one or more different surface species, and by 200 K this conversion is complete. The same conversion occurs if the surface represented by Figure 5, c or d, is annealed, but at slightly higher temperatures; the conversion is complete by 215 K following a 2-L formamide exposure and by 230 K following a 4-L exposure. The EEL spectrum measured after annealing the surface of Figure 5a to 200 K is shown in Figure 6a, and it is obviously very similar (but not identical) to the EEL spectrum of  $\eta^2(\text{C,O})\text{-NH}_2\text{CO}$  on clean Ru(001) that is shown in Figure 6b. The intense  $\nu(\text{CO})$  loss feature of  $\eta^1(\text{O})\text{-NH}_2\text{CHO}$  at 1660  $\text{cm}^{-1}$  has disappeared completely, while a loss feature remains at 1585  $\text{cm}^{-1}$  that is considerably stronger than the  $\delta(\text{NH}_2)$  loss feature of  $\eta^1(\text{O})\text{-NH}_2\text{CHO}$ . The intense  $\delta(\text{NCO})$  mode of  $\eta^1(\text{O})\text{-NH}_2\text{CHO}$  has disappeared also, leaving a broad peak near 445  $\text{cm}^{-1}$ , a weak peak at 300  $\text{cm}^{-1}$ , and two rather intense peaks at 655 and 825  $\text{cm}^{-1}$ . Loss features due to nitrogen-hydrogen and carbon-hydrogen stretching vibrations are present near 3335 and 2885  $\text{cm}^{-1}$ , respectively. [The latter is almost certainly not a "softened" NH stretching mode, since no such vibration was observed following formamide adsorption on clean Ru(001) under any circumstances.] Additional loss features are present at 1395, 1300, 1135, and 1015  $\text{cm}^{-1}$ , with the last peak being very weak. The intensity of the 1135- $\text{cm}^{-1}$  peak is due partially to  $\nu_s(\text{RuH})$  of hydrogen adatoms.

While the EEL spectrum of Figure 6a is clearly similar to that of  $\eta^2(\text{C,O})\text{-NH}_2\text{CO}$  on clean Ru(001), a significant difference is the presence of the  $\nu(\text{CH})$  loss feature at 2885  $\text{cm}^{-1}$ , indicating that a species containing a carbon-hydrogen bond is present on

(45) For sufficiently high initial formamide coverages, some molecular desorption is observed also.

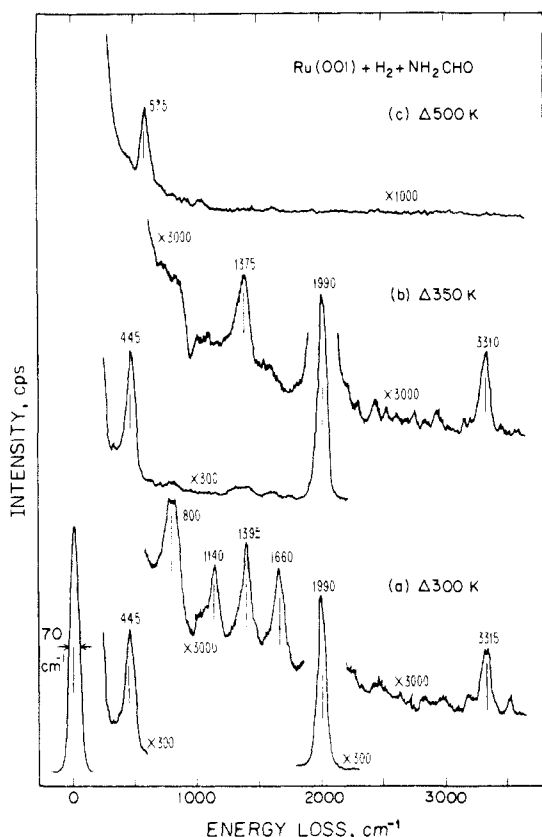


Figure 7. The EEL spectra that result when a hydrogen-presaturated Ru(001) surface is exposed to 0.5 L of  $\text{NH}_2\text{CHO}$  at 80 K and then annealed to (a) 300 K, (b) 350 K, and (c) 500 K.

the surface. Since this mode is not observed in the case of  $\eta^2(\text{C},\text{O})\text{-NH}_2\text{CO}$  on clean Ru(001) and because it loses little intensity in spectra measured  $10^\circ$  off-specular,<sup>46</sup> it cannot be assigned as a combination band of the modes with loss features at 1300 and 1585  $\text{cm}^{-1}$ , and the lack of the intense  $\nu(\text{CO})$  loss feature at 1660  $\text{cm}^{-1}$  indicates that it cannot be due either to the presence of  $\eta^1(\text{O})\text{-NH}_2\text{CHO}$  or to any other formamide species that maintains the carbonyl double bond. It is therefore attributed to  $\eta^2(\text{C},\text{O})\text{-NH}_2\text{CHO}$ , which is stabilized by the presence of coadsorbed hydrogen. Some  $\eta^2(\text{C},\text{O})\text{-NH}_2\text{CHO}$  may also be present on the surface represented by Figure 6a; since these two species are expected to have rather similar EEL spectra, a clear distinction between the two cannot be made. The mode assignments for  $\eta^2(\text{C},\text{O})\text{-NH}_2\text{CO}$  on clean Ru(001) are listed in Table I along with those for  $\eta^2(\text{C},\text{O})\text{-NH}_2\text{CHO}$  from Figure 6a, and the EEL spectrum of Figure 6a is discussed further in section IV.

Annealing the surface to 250 K (cf. Figure 6c) results in the disappearance of the  $\nu(\text{CH})$  loss feature, indicating that the conversion of all of the  $\eta^2(\text{C},\text{O})\text{-NH}_2\text{CHO}$  to  $\eta^2(\text{C},\text{O})\text{-NH}_2\text{CO}$  has gone to completion. The intensity of the carbon monoxide loss feature at 1975  $\text{cm}^{-1}$  has increased significantly, suggesting that approximately 0.01 monolayer of  $\eta^2(\text{C},\text{O})\text{-NH}_2\text{CHO}$  has decomposed to carbon monoxide, NH, and hydrogen adatoms (vide infra). In addition, the loss features at 825 and 1135  $\text{cm}^{-1}$  have decreased somewhat in intensity relative to the other loss features in the spectrum. After annealing the surface to 300 K, all loss features due to  $\eta^2(\text{C},\text{O})\text{-NH}_2\text{CHO}$  have disappeared completely. This is true for all formamide coverages.

Figure 7a–c show the EEL spectra obtained after annealing the same surface to 300, 350, and 500 K, respectively. Figure

7c shows only a single loss feature at 575  $\text{cm}^{-1}$  due to  $\nu_s(\text{RuN})$  of nitrogen adatoms, consistent with the thermal desorption results which indicate that only nitrogen desorbs from the surface above 500 K. Since this loss feature disappears upon annealing to 850 K, its identification with nitrogen adatoms is unambiguous. The spectra of Figure 7 measured after annealing the surface to 300 and 350 K show intense loss features at 445 and 1900  $\text{cm}^{-1}$ , which are due to  $\nu(\text{Ru-CO})$  and  $\nu(\text{CO})$  of approximately 0.03 monolayer of carbon monoxide.<sup>47</sup> In addition, Figure 7a shows losses at 800, 1140, 1395, 1660, and 3315  $\text{cm}^{-1}$ , and Figure 7b shows losses at 1375 and 3310  $\text{cm}^{-1}$ . The loss features near 3310 and 1375  $\text{cm}^{-1}$  disappear concomitantly near 400 K, and are assigned to  $\nu(\text{NH})$  and  $\delta(\text{NH})$ , respectively, of an NH species, in accordance with our previous results for formamide decomposition on clean Ru(001).<sup>2</sup> The disappearance of these loss features upon annealing to 400 K correlates with the appearance of the 575- $\text{cm}^{-1}$  loss feature, indicating that the NH decomposes to nitrogen and hydrogen adatoms as on clean Ru(001).<sup>2</sup> The loss features at 800 and 1140  $\text{cm}^{-1}$  are attenuated greatly upon annealing from 300 to 350 K, and are due primarily to the presence of hydrogen adatoms. The 1660- $\text{cm}^{-1}$  loss feature is assigned to  $\nu(\text{CO})$  of a small amount of  $\eta^1(\text{O})\text{-NH}_2\text{CHO}$  that is readsorbed from the chamber background, in agreement with our previous results for formamide adsorption on Ru(001)- $p(1\times 2)\text{-O}$ .<sup>4</sup> Note that such a small amount of  $\eta^1(\text{O})\text{-NH}_2\text{CHO}$  could be present in any of the EEL spectra of Figure 6 and would be barely detectable due to overlap with the loss feature near 1590  $\text{cm}^{-1}$ . In summary, our EELS results indicate that the stable decomposition products of  $\eta^2(\text{C},\text{O})\text{-NH}_2\text{CO}$  on hydrogen-presaturated Ru(001) are CO, NH, and hydrogen adatoms. As on clean Ru(001),<sup>2</sup> there is no evidence for the formation of a stable NH<sub>2</sub> species, although the possibility that very small amounts of NH<sub>2</sub> might be present cannot be ruled out completely based on the EELS data alone.

#### IV. Discussion

On hydrogen-presaturated Ru(001) at 80 K, formamide adsorbs molecularly through a lone pair of electrons on the oxygen atom in an  $\eta^1(\text{O})$ -bonded configuration. The bonding of  $\eta^1(\text{O})\text{-NH}_2\text{CHO}$  to the surface may be thought of as a Lewis acid–Lewis base interaction, with the surface acting as a Lewis acid and the formamide as a Lewis base. This  $\eta^1(\text{O})\text{-NH}_2\text{CHO}$  is the same molecular species that is formed on Ru(001)- $p(1\times 2)\text{-O}$  at 80 K<sup>34</sup> and is quite different from the  $\eta^2(\text{C},\text{O})\text{-NH}_2\text{CO}$  which is formed following low exposures of formamide on clean Ru(001) at 80 K. Thus, the preadsorption of hydrogen makes a quantitative difference in the bonding of formamide on Ru(001) at 80 K, just as the preadsorption of oxygen does.

It is of interest that both a saturation hydrogen coverage ( $\theta_{\text{H}} \sim 0.85$ ) and an ordered  $p(1\times 2)$  overlayer of oxygen adatoms ( $\theta_{\text{O}} = 0.5$ ) cause the same alteration of the bonding of formamide to Ru(001) at 80 K (compared with the clean surface). The fact that  $\eta^1(\text{O})\text{-NH}_2\text{CHO}$  is formed on hydrogen-presaturated Ru(001) rather than  $\eta^2(\text{C},\text{O})$ -bonded species indicates that the hydrogen adatoms increase the activation barrier for the formation of  $\eta^2(\text{C},\text{O})$ -bonded species. A priori, this increased activation barrier could result from either steric or electronic effects, or a combination of both. Due to the very similar electronegativities of ruthenium (2.2) and hydrogen (2.1),<sup>47</sup> the adsorption of hydrogen has only a small effect on the work function of the Ru(001) surface; a saturation hydrogen coverage at 95 K causes the work function to decrease by only 10 meV.<sup>9</sup> This is in contrast to the formation of a  $p(1\times 2)$  oxygen adatom overlayer on Ru(001), which causes the work function of this surface to increase by 1.06 eV<sup>48</sup> and thus favors strongly lone pair donor bonding [e.g.,  $\eta^1(\text{O})$ -bonding] over  $\eta^2(\text{C},\text{O})$ -bonding, the latter of which involves significant electron back-donation from the surface metal atoms to the  $\pi^*$  orbital(s) of the ligand. This suggests that the effects of preadsorbed hydrogen are primarily steric, and that hydrogen

(46) Vibrational modes that are primarily impact excited, including virtually all hydrogenic stretching modes, are approximately as strong in off-specular EEL spectra as in specular EEL spectra. This is in contrast to modes that are primarily dipole excited (and combination bands of such modes), which are much stronger on-specular. See: Ibach, H.; Mills, D. L. In *Electron Energy Loss Spectroscopy and Surface Vibrations*; Academic: New York, 1982, Chapters 1 and 3.

(47) Jolly, W. L. In *The Principles of Inorganic Chemistry*; McGraw-Hill: New York, 1976; p 43.

(48) Madey, T. E.; Engelhardt, H. A.; Menzel, D. *Surf. Sci.* **1975**, *48*, 304.

diffusion on the surface is the key factor in permitting the  $\eta^1(\text{O})$ -formamide-to- $\eta^2(\text{C},\text{O})$ -formamide conversion to occur. However, electronic effects cannot be excluded completely; the bonding of a nearly complete monolayer of hydrogen adatoms to the surface might reduce the *local* density of states at the Fermi level to the point where CO bond rehybridization is no longer favorable at 80 K.

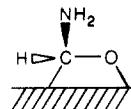
It should be noted that while the same  $\eta^1(\text{O})$ -NH<sub>2</sub>CHO species is formed on hydrogen-presaturated Ru(001) and Ru(001)-p(1×2)-O at 80 K, different decomposition products of this species are observed in each case which can be correlated with the different perturbations of the ruthenium by the hydrogen and the oxygen. On the hydrogen-presaturated surface, where the separation between the Fermi level and the formamide  $\pi^*$  orbital is 1.07 eV less than on the oxygen-precovered surface, the  $\eta^1(\text{O})$ -NH<sub>2</sub>CHO converts to  $\eta^2(\text{C},\text{O})$ -NH<sub>2</sub>CHO, which undergoes significant carbon-oxygen bond rehybridization that results in part from electron back-donation from the metal to the formamide  $\pi^*$  orbital. On the other hand,  $\eta^1(\text{O})$ -NH<sub>2</sub>CHO on Ru(001)-p(1×2)-O converts to  $\eta^2(\text{N},\text{O})$ -NH<sub>2</sub>CHO, which bonds to the surface via lone pair donor bonds on both the oxygen and nitrogen atoms. Thus, on hydrogen-presaturated Ru(001), the  $\eta^1(\text{O})$ -NH<sub>2</sub>CHO converts to the molecularly adsorbed species with the greatest metal-to-formamide charge transfer, while on Ru(001)-p(1×2)-O it converts to the molecularly adsorbed species with the greatest formamide-to-metal charge transfer.

The conversion of the initially adsorbed  $\eta^1$ -formamide species to  $\eta^2(\text{C},\text{O})$ -bonded species is in agreement with our previous assignment of the former as being  $\eta^1(\text{O})$ -bonded rather than  $\eta^1(\text{N})$ -bonded, since the conversion of an  $\eta^1(\text{N})$ -bonded to an  $\eta^2(\text{C},\text{O})$ -bonded species is unlikely. The  $\eta^1(\text{O})$ -bonding configuration is expected to be favored over  $\eta^1(\text{N})$ -bonding for molecular formamide, because in the gas-phase molecule there is no electron lone pair strictly localized on the nitrogen atom due to the partial double bond character of the carbon-nitrogen bond. It has been noted previously<sup>4</sup> that the observed  $\nu(\text{CO})$  frequency of the  $\eta^1$ -bonded formamide of approximately 1670 cm<sup>-1</sup>, which is substantially reduced from the gas-phase value of 1734 cm<sup>-1</sup>,<sup>44</sup> provides additional support for  $\eta^1(\text{O})$ -bonding. This is in agreement with IR data for the organometallic compounds *trans*-PtCl<sub>2</sub>(C<sub>2</sub>H<sub>4</sub>)(NH<sub>2</sub>CONH<sub>2</sub>) and *trans*-PtCl<sub>2</sub>(C<sub>2</sub>H<sub>4</sub>)-[(CH<sub>3</sub>)<sub>2</sub>NCHO], where a decrease in the frequency of  $\nu(\text{CO})$  upon coordination was observed for both urea and dimethylformamide, and was taken as evidence that the urea and dimethylformamide ligands are O-bonded rather than N-bonded.<sup>14</sup> In contrast, the N-bonded urea ligands in *trans*-PtCl<sub>2</sub>(urea)<sub>2</sub> exhibit  $\nu(\text{CO})$  at 1725 cm<sup>-1</sup>, 46 cm<sup>-1</sup> higher than  $\nu(\text{CO})$  in free urea.<sup>14</sup>

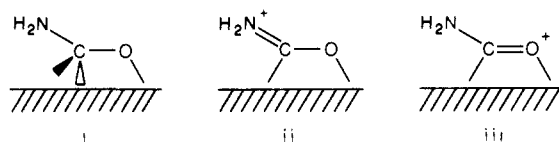
The EEL spectra that were measured following annealing of the hydrogen-saturated Ru(001) surface with a few hundredths of a monolayer of adsorbed  $\eta^1(\text{O})$ -NH<sub>2</sub>CHO to 200 K (cf. Figure 6a) are quite similar to those of  $\eta^2(\text{C},\text{O})$ -NH<sub>2</sub>CO on clean Ru(001),<sup>2</sup> but a significant difference is the presence of the loss feature at 2885 cm<sup>-1</sup> due to a carbon-hydrogen stretching mode. This indicates that a species containing a carbon-hydrogen bond is present, and since the  $\nu(\text{CH})$  loss feature is as strong as that in Figure 5a while the strong modes at 1660 and 525 cm<sup>-1</sup> have disappeared completely, it cannot be attributed to residual  $\eta^1(\text{O})$ -NH<sub>2</sub>CHO. Possible decomposition products of formamide that contain carbon-hydrogen bonds also cannot account for this loss feature. For example, the observed frequency of 2885 cm<sup>-1</sup> is approximately 100 cm<sup>-1</sup> lower than the  $\nu(\text{CH})$  frequencies of methylidyne<sup>49,50</sup> and  $\eta^2(\text{C},\text{O})$ -NHCHO (and the remainder of the EEL spectrum of Figure 6a is not consistent with the latter).<sup>3,4</sup> No strong loss feature is observed between approximately 1700 and 1800 cm<sup>-1</sup>, as would be expected for either  $\eta^1(\text{N})$ -NCHO or  $\eta^1(\text{N})$ -NHCHO.<sup>33</sup> A formyl (CHO) species is not expected to be stable on Ru(001) at 200 K, since  $\eta^1(\text{C})$ -HCO was not observed

in the decomposition of formaldehyde on Ru(001) at 80 K,<sup>36</sup> and  $\eta^2(\text{C},\text{O})$ -HCO is not stable above 120 K on this surface.<sup>36</sup> In addition, there is no evidence for the production of NH<sub>3</sub> or NH at or below 200 K. Thus, this loss feature is interpreted as being due to the presence of  $\eta^2(\text{C},\text{O})$ -NH<sub>2</sub>CHO, which is stabilized with respect to carbon-hydrogen bond cleavage by the large concentration of hydrogen adatoms on the surface.

The EEL spectrum of  $\eta^2(\text{C},\text{O})$ -NH<sub>2</sub>CHO is expected to be similar to that of  $\eta^2(\text{C},\text{O})$ -NH<sub>2</sub>CO, though not identical. Only a single resonance structure can be written for di- $\sigma$ -bonded  $\eta^2(\text{C},\text{O})$ -NH<sub>2</sub>CHO, and the carbon-nitrogen and carbon-oxygen bonds are expected to be pure single bonds:



A  $\pi$ -bonded structure containing a carbon-oxygen double bond is also possible for  $\eta^2(\text{C},\text{O})$ -NH<sub>2</sub>CHO, but is not expected to contribute significantly to the actual structure of this ligand on the ruthenium surface. On the other hand, three different resonance structures can contribute to the structure of  $\eta^2(\text{C},\text{O})$ -NH<sub>2</sub>CO:



Thus  $\eta^2(\text{C},\text{O})$ -NH<sub>2</sub>CHO is expected to have lower  $\nu(\text{CN})$  and  $\nu(\text{CO})$  frequencies than  $\eta^2(\text{C},\text{O})$ -NH<sub>2</sub>CO, and probably also differing amounts of coupling of these modes to the various NH<sub>2</sub> deformation modes [e.g., less coupling to  $\delta(\text{NH}_2)$  near 1585 cm<sup>-1</sup> and more to  $\omega(\text{NH}_2)$  near 820 cm<sup>-1</sup>]. Since the EEL spectrum of Figure 6a is so similar to that of  $\eta^2(\text{C},\text{O})$ -NH<sub>2</sub>CO on clean Ru(001) (Figure 6b), one possible interpretation of this spectrum is that it is due to a mixture of  $\eta^2(\text{C},\text{O})$ -NH<sub>2</sub>CO and  $\eta^2(\text{C},\text{O})$ -NH<sub>2</sub>CHO. Another possibility, however, is that resonance structure i is by far the most important in the actual structure of  $\eta^2(\text{C},\text{O})$ -NH<sub>2</sub>CHO, so that the carbon-oxygen and carbon-nitrogen bonds are essentially single bonds in both surface species. This could lead to very similar EEL spectra for the two  $\eta^2(\text{C},\text{O})$ -bonded species, because the only modes that would be dipolar-allowed for  $\eta^2(\text{C},\text{O})$ -NH<sub>2</sub>CHO but not for  $\eta^2(\text{C},\text{O})$ -NH<sub>2</sub>CO are some of the hydrogenic modes, and, with the exception of  $\omega(\text{NH}_2)$  (which would be dipolar-allowed for both species), these modes are expected to have only very weak dynamic dipoles. The marked changes in the frequencies and intensities of the ruthenium-ligand stretching modes below 500 cm<sup>-1</sup> on the hydrogen-presaturated surface compared with the clean surface no doubt result from both the different bonding geometry of  $\eta^2(\text{C},\text{O})$ -NH<sub>2</sub>CHO compared with  $\eta^2(\text{C},\text{O})$ -NH<sub>2</sub>CO and a perturbation of the bonding of both species on the hydrogen-presaturated surface caused by the coadsorbed hydrogen adatoms.

Further annealing of the surface, which has been exposed to 0.5 L of formamide, to 250 K reduces the  $\nu(\text{CH})$  loss feature to the level of noise, consistent with the complete conversion of the  $\eta^2(\text{C},\text{O})$ -NH<sub>2</sub>CHO to  $\eta^2(\text{C},\text{O})$ -NH<sub>2</sub>CO. The increase in the intensity of the loss feature due to  $\nu(\text{CO})$  of carbon monoxide indicates that some of the  $\eta^2(\text{C},\text{O})$ -NH<sub>2</sub>CO (approximately 0.01 monolayer) has decomposed to CO, NH, and hydrogen adatoms. The decrease in the intensity of the 1135-cm<sup>-1</sup> loss feature upon annealing from 200 to 250 K suggests that at 200 K this mode derives most of its intensity from a carbon-hydrogen bending mode of  $\eta^2(\text{C},\text{O})$ -NH<sub>2</sub>CHO rather than from  $\nu(\text{RuH})$  of hydrogen adatoms, since very little surface hydrogen desorbs below 250 K. The decomposition of  $\eta^2(\text{C},\text{O})$ -NH<sub>2</sub>CO to CO, NH, and hydrogen adatoms is complete after annealing to 300 K. Low coverages ( $\theta < 0.05$ ) of  $\eta^2(\text{C},\text{O})$ -NH<sub>2</sub>CO on Ru(001) are thus stabilized slightly by the presence of hydrogen adatoms, since the decomposition of a similar coverage of  $\eta^2(\text{C},\text{O})$ -NH<sub>2</sub>CO on clean Ru(001) is complete by 250 K.<sup>2</sup> However, for a saturation coverage

(49) Hills, M. M.; Parmeter, J. E.; Mullins, C. B.; Weinberg, W. H. *J. Am. Chem. Soc.* **1986**, *108*, 3554.

(50) Parmeter, J. E.; Hills, M. M.; Weinberg, W. H. *J. Am. Chem. Soc.* **1986**, *108*, 3563.

